RECENT IRRADIATION TESTS OF URANIUM-PLUTONIUM-ZIRCONIUM METAL FUEL ELEMENTS*

CONF-860931--9

DE87 004980

by

R. G. Pahl, C. E. Lahm, and
R. Villarreal

Argonne National Laboratory
P.O. Box 2528
Idaho Falls, ID 83403-2528

G. L. Hofman, and W. N. Beck

9700 South Cass Avenue
Argonne, IL 60439

Paper to be Presented

at

International Conference on Reliable Fuels for Liquid Metal Reactors

Tucson, Arizona

September 7-11, 1986

*Work Supported by the U.S. Department of Energy Reactor Systems, Development, and Technology, Under Contract W-31-109-ENG-38

RECENT IRRADIATION TESTS OF URANIUM-PLUTONIUM-ZIRCONIUM METAL FUEL ELEMENTS*

R. G. Pahl, C. E. Lahm, R. Villareal
Argonne National Laboratory
P.O. Box 2528
Idaho Falls, ID 83403-2528
(208) 526-7572, -7036, -7311

W. N. Beck, G. L. Hofman
Argonne National Laboratory
9700 S. Cass Avenue
Argonne, IL 60439
(312) 972-6675, -6683

ABSTRACT

Uranium-Plutonium-Zirconium metal fuel irradiation tests to support the ANL Integral Fast Reactor concept are discussed. Satisfactory performance has been demonstrated to 2.9 at.% peak burnup in three alloys having 0, 8, and 19 wt % plutonium. Fuel swelling measurements at low burnup in alloys to 26 wt % plutonium show that fuel deformation is primarily radial in direction. Increasing the plutonium content in the fuel diminishes the rate of fuel-cladding gap closure and axial fuel column growth. Chemical redistribution occurs by 2.1 at.% peak burnup and generally involves the inward migration of zirconium and outward migration of uranium. Fission gas release to the plenum ranges from 46% to 56% in the alloys irradiated to 2.9 at.% peak burnup. No evidence of deleterious fuel-cladding chemical or mechanical interaction was observed.

* Work supported by the U.S. Department of Energy, Reactor Systems, Development and Technology, under Contract W-31-109-Eng-38.

RECENT IRRADIATION TESTS OF URANIUM-PLUTONIUM-ZIRCONIUM METAL FUEL ELEMENTS*

I. INTRODUCTION

Argonne National Laboratory's Integral Fast Reactor (IFR) concept is a complete fuel cycle which is based on a pool-type reactor, sodium cooled and fueled with the U-Pu-Zr alloy. One of the first steps undertaken to demonstrate technical feasibility of the concept involved an ongoing series of irradiation tests performed in the Experimental Breeder Reactor II (EBR-II). The purpose of this paper will be to outline the scope of these tests and to share the results of our latest post-irradiation examinations (PIE) at low burnup.

An IFR will use a uranium-plutonium alloy fuel which contains about 10% zirconium by weight. The zirconium provides an elevated fuel solidus temperature and good chemical compatibility with the stainless steel cladding. The initial core loading of an IFR on startup will consist of binary U-10Zr fuel which has been suitably enriched in U-235. Plutonium that is bred in the core and blanket region will eventually provide the fissile content necessary to sustain reactivity through the lifetime of the reactor. The existing fuel performance data base for U-Pu-Zr fuel, exclusive of the current data presented herein, is limited to about 40 fuel elements irradiated in EBR-II and the CP-5 thermal reactor in the 1960's. Peak burnups of about 4.5 at.% (heavy metal) had been achieved by the time the original program was phased out in favor of oxide-fuel development, but one test involving U-19Pu-14Zr fuel did reach 12.5 at.% burnup without breach in CP-5. While our prior experience with U-Pu-Zr fuel is limited, our knowledge of metallic fuel behavior in general is not. The EBR-II has operated successfully with metallic driver fuel* since 1964 and upwards of 150,000 Mark-II elements have been irradiated. The development of EBR-II metallic driver fuel as a viable fuel-element type is the subject of a companion paper in these proceedings.[1] It should be noted that standard Mark-II fuel is currently being consumed in EBR-II at the rate of almost 5000 elements per year and can routinely achieve 10 at.% burnup without breach.

The irradiation tests described in this paper were designed to build upon our extensive EBR-II metallic fuel data base, and to extend our knowledge of U-Pu-Zr fuel performance to high burnup using more prototypal designs and operating conditions.

II. EXPERIMENTAL PROGRAM

A total of five subassemblies have been irradiated to date in support of the IFR concept. In February of 1985 three 61-pin subassemblies (X419, X420,

* The driver fuel alloy used in EBR-II is U-5Fs (wt %) where Fs or "fissium" is nominally 2.5% Mo, 1.9 % Ru, 0.3% Rh, 0.2% Pd, 0.1% Zr, and 0.01%Nb. This mixture of fission products is the equilibrum composition of fuel which has been pyrometallurgically reprocessed in the EBR-II Fuel Cycle Demonstration of the 1960's.

and X421) began operation in the EBR-II reactor. A fourth subassembly (X423) containing 37 pins began operation in July of 1985, while the latest 61-pin subassembly (X425) began its irradiation in February 1986. The lead subassembly, X421, has achieved a peak burnup of 5.9 at.% as of April 1986. The tests spanned a wide range of pin powers, cladding temperatures, and fuel compositions. Details on their specific design and operation characteristics are summarized below.

A. Element Design

The basic element design common to all five tests incorporates features which have evolved through the design progressions of EBR-II driver fuel. In all cases, the fuel slug is a single solid cylinder 343 mm (13.5 in.) in length which has been injection-cast into precision-bore, disposable quartz molds by pressurizing the vacuum furnace with high-purity argon. This casting method is used for EBR-II driver-fuel production and produces sound, homogeneous fuel with high yields.

The fuel is sodium bonded within the seamless stainless steel cladding, which after closure TIG-welding are wrapped with a helical pitch spacer wire. The plenum gas is nominally 25% Ar, 75% He, spiked with a known isotopic mixture of Xenon for purposes of in-reactor breach detection.

The fuel composition has been varied to be representative of the changing plutonium content which builds up at each reprocessing step in the IFR fuel cycle concept. Subassemblies X419, X420, X421, and X425 contain only U-10Zr, U-8Pu-10Zr, and U-10Pu-10Zr fuel (wt %), respectively, while subassembly X423 contains fuel of composition U-XPu-10Zr where X = 0, 3, 8, 19, 22, and 26 wt % plutonium. In all cases, the U-235 enrichment has been adjusted for the difference in plutonium content so that all pins within a given subassembly operate at equal linear power ratings.

Three cladding types have been investigated and were chosen for their known irradiation properties as well as their availability and fabricability. Two 20% cold-worked austenitic stainless steel alloys were chosen, AISI 316 and D9 (UNS S38660) as well as a martensitic stainless steel, HT9 (modified AISI 422).

Table 1 summarizes the important design features of the elements.

B. Operating Conditions

EBR-II's steady-state operation at 58.5 MWt consists of cycles or "runs" which are six to seven weeks in duration followed by fuel handling/maintenance shutdowns which average one to two weeks. The five subassemblies identified above were irradiated in rows-3 and -4 of the reactor core. The peak operating conditions for the five subassemblies, as predicted by the EBR-II transport code GODZILLA-DOT and HECTIC heat transfer code are shown in Table 2 using beginning-of-life materials properties.

III. RESULTS OF POST-IRRADIATION EXAMINATIONS

A. Fuel Swelling

Fuel deformation at low burnup is driven by the internal pressure of fission gas bubbles while solid fission product accumulation does contribute

TABLE 1

Nominal Design Features of the Fuel Elements

Subassembly Type	D-61 (61 pins)	D-37 (37 pins)
Subassembly No.	X419,X420,X421,X425	X423
Fuel Alloys, U-XPu-10Zr, (wt.%)	X = 0,8,19	X = 0,3,8,19,22,26
Fuel Enrichment, % U^{235}/U^{total}	69,64.5,57	37,34,29,16,13,6
Fuel Slug Length, mm (in.)	343 (13.5)	343 (13.5)
Fuel Slug Diameter, mm (in.)	4.32 (.170)	5.66 (.223)
Fuel Slug Mass, gms	78.	136.
Sodium Fill Above Fuel, mm (in.)	6.35 (.25)	6.35 (.25)
Cladding Type	D9 (20% CW) or HT9 (SA,T)	316 (20% CW)
Cladding Outer Diameter, mm (in.)	5.84 (.230)	7.37 (.290)
Cladding Wall Thickness, mm (in.)	.381 (.015)	.406 (.016)
Spacer Wire Diameter, mm (in.)	1.07 (.042)	1.44 (.057)
Spacer Wire Pitch, mm (in.)	152. (6.00)	152. (6.00)
Fuel Element Mass, gms	122	202
Fuel:Plenum Volume Ratio (25°C)	1.01	1.07

TABLE 2

Peak Operating Conditions for the 3 Element Types*

Element Power Rating, W/cm (kW/ft)	D9:	482	(14.7)
	HT9:	397	(12.1)
	316SS:	413	(12.6)
Fuel Centerline Temperature, °C (°F)	D9:	729	(1344)
	HT9:	741	(1366)
	316SS:	641	(1186)
Fuel Surface Temperature, °C (°F)	D9:	595	(1103)
	HT9:	611	(1132)
	316SS:	533	(991)
Cladding Inside Wall Temperature, °C (°F)	D9:	583	(1081)
	HT9:	600	(1112)
	316SS:	522	(972)
Cladding Outside Wall Temperature, °C (°F)	D9:	541	(1006)
	HT9:	558	(1036)
	316SS:	488	(910)

* Tabulated parameters are the maximum claculated for the five experimental subassemblies in the irradiation period from 2/85 to 5/86, (EBR-II reactor runs #133 to #138). Beginning-of-life fuel and cladding properties have been used. The wide range of operating conditions tabulated is primarily a consequence of the ~30% step-change in flow between rows 3 and 4 of the EBR-II.

at higher burnup. The fuel elements in these tests have been designed with smear-densities (fuel cross-sectional area divided by available inside cladding area) in the range of 72 to 75% so that fuel area deformation of 33 to 38% can be accommodated prior to fuel/cladding contact. This design feature has been the key to achieving high burnup in the Mark-II driver-fuel elements used in the EBR-II. The development of interconnected porosity in the fuel promotes the release of fission gas to the plenum region, thus mitigating significant fuel/cladding contact stresses prior to significant solid fission product buildup in the fuel. Fuel swelling in such low smear-density designs allows dynamic and repeated swelling of the matrix into the continually developing and decaying interconnected porosity.

In the discussion which follows, fuel swelling has been reported in terms of engineering strain and was calculated from the change between as-built dimensions and those taken from neutron-radiography data after irradiation. Precision measurements of the as-irradiated fuel slug diameters prior to cladding contact were accomplished with a Bausch and Lomb quantitative image analysis system.

Fuel swelling in all of the alloys tested is primarily radial. Neutron radiographs of elements from subassembly X423 (at 0.44 and 0.89 at.% peak burnup) were examined. Figures 1 and 2 show that the diametral strain [averaged over the entire fuel column at discrete 2.5 mm (.10 in.) intervals] is always greater than fuel column elongation by a factor of 1.3 to 2.8 depending on burnup and alloy. Fuel cladding contact is essentially complete between 0.89 and 2.1 at.% peak burnup.

Figure 3 illustrates the burnup dependence of average fuel column elongation for the U-10Zr, U-8Pu-10Zr, and U-19Pu-10Zr alloys. The decrease in growth rate beyond ~1 at.% burnup presumably coincides with fuel/cladding contact and the slight fuel-column shrinkage beyond ~2 at.% burnup suggests that the axial growth may be ultimately self-limiting. The strong dependence of fuel swelling on plutonium content has been observed consistently in subassemblies X423 and X419, and the basic reasons behind this effect are currently being investigated in terms of the irradiation creep strength of the alloys involved. Axial fuel growth in all alloys has been found to be independent of fuel temperature (within a fuel element bundle) with the exception of the U-19Pu-10Zr alloy. The data from X419 at ~2.1 and 2.9 at.% peak burnup shows that a two-fold increase in axial growth occurred below about 575°C average fuel temperature (using beginning-of-life properties).

B. Fuel Restructuring

Preliminary metallography of the six fuel alloys from X423 at 0.44 at.% peak burnup shows little discernable change in microstructure with irradiation. However, more detailed optical metallography has been performed on the U-10Zr, U-8Pu-10Zr, and U-19Pu-10Zr fuel from X419 at 2.1 at.% peak burnup, with some preliminary work now complete at 2.9 at.% peak burnup. Extensive fuel restructuring has been observed at the 2.1 at.% peak burnup level in all 3 alloys and is discussed separately below.

1. U-10Zr. The as-polished metallographic sections of Fig. 4 show that, as stated earlier, complete fuel/cladding gap closure has taken place [initially .76 mm (.30 in.) diametral clearance]. The micrograph taken at the bottom of the fuel column shows the extreme plasticity of the U-10Zr fuel at

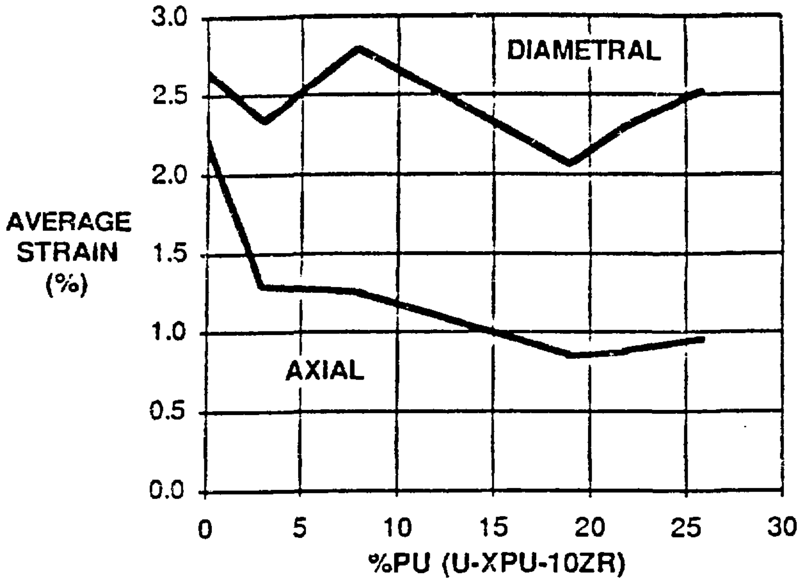

Figure 1. Plutonium Dependence of Fuel Deformation at 0.44 at.% Peak Burnup.

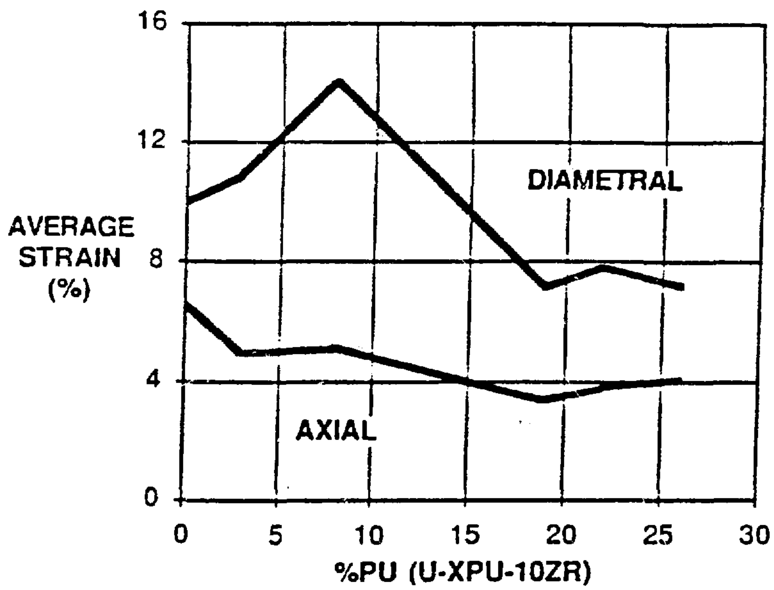

Figure 2. Plutonium Dependence of Fuel Deformation at 0.89 at.% Peak Burnup.

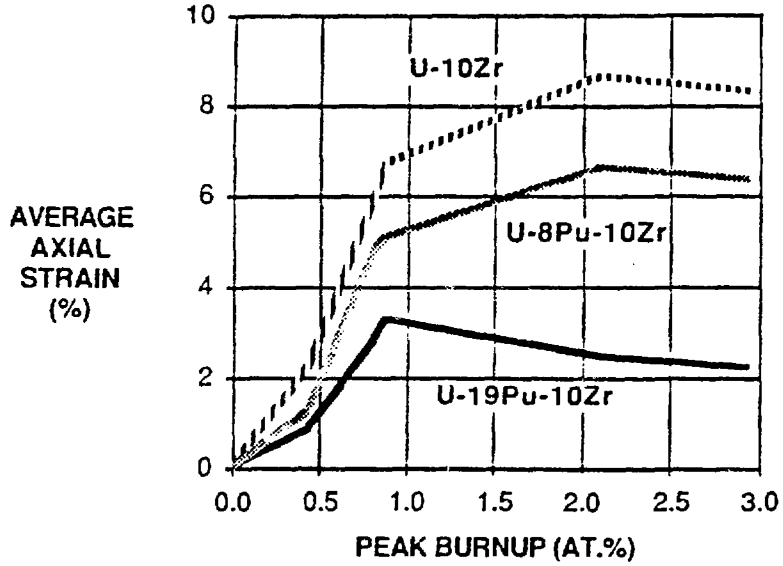

Figure 3. Burnup Dependence of Fuel Column Elongation for the 0, 8, and 19 wt % Pu Alloys.

this level of burnup. The internal pressure of the fission gas bubbles has caused extrusion of the fuel into the annular recess which has been machined on the bottom closure plug. This type of behavior is consistent with the high swelling rate that this alloy exhibits. Uniform fission-gas bubble distributions are found only at the lower end of the fuel slug.

The "bullseye" effect that appears on transverse sections above core midplane is due to annular bands of differing porority which may correspond to isotherm and/or isocomposition surfaces in the fuel. Quantitative metallography of the midplane and topmost transverse section show local variations in areal pore coverage ranging from 20 to 80%. Restructuring of the U-10Zr fuel is not limited to the visible bands of porosity, however. Microchemical analysis has shown that chemical redistribution has also taken place during the 7.34×10^6 sec (85 days) at full power. A ~6.4 mm (0.25-in.) longitudinal section of fuel near midplane was electrodischarge machined (EDM) (spark eroded) into 14 concentric samples and analyzed by isotopic dilution mass-spectrometry for uranium and for zirconium by spectrophotometric techniques. The light-colored band of low porosity that is visible at X/R = 0.5 on the midplane section has the approximate composition of U-5Zr. Slight enrichment of zirconium was evident immediately adjacent to the cladding. The migration of zirconium in-reactor has important performance implications since it provides a high solidus temperature and good cladding-compatibility. Zirconium migration toward the fuel centerline of U-Pu-Zr fuel was also observed in the early irradiation tests of the 1960's. Interdiffusion of fuel components in-reactor is a complex phenomena due to the superposition of temperature gradients and flux effects. A joint effort between Argonne National

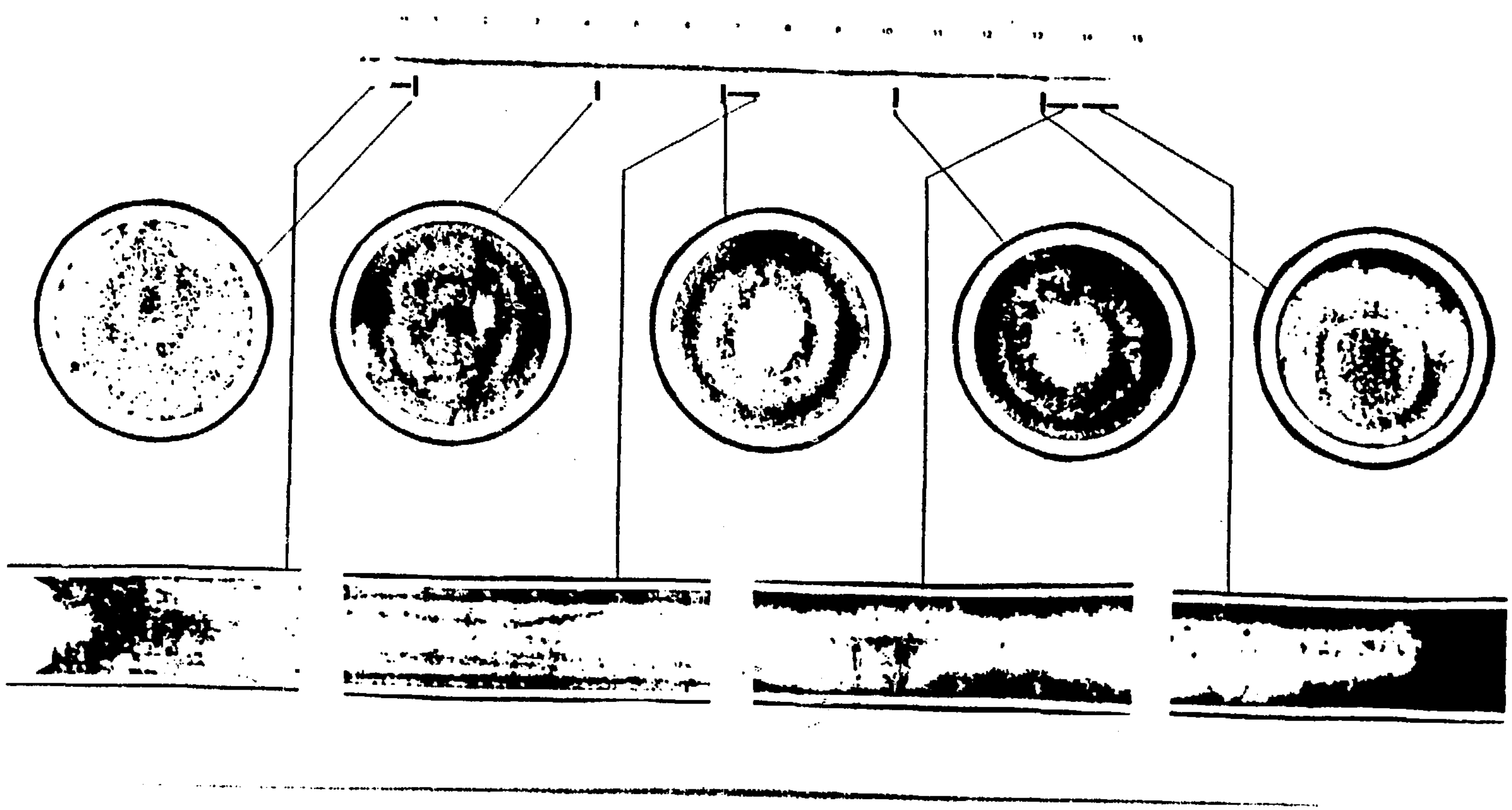

Figure 4. U-10Zr Fuel Microstructure at 2.1 at.% Peak Burnup.

Laboratory and Purdue University is currently underway to understand this phenomena in binary and ternary U-Pu-Zr alloys.

One microstructural feature observed on the surface of all as-cast fuel alloys was a thin [0.025 mm (0.001 in.)] discontinuous layer of zirconium-rich material which presumably resulted from the interaction between fuel and mold-wash. The mold-wash is ZrO_2 powder (1 to 4 microns diameter) applied to protect the inside wall of the quartz molds during fuel solidification. This discontinuous layer was also observed in the irradiated fuel but had little effect at the 2.1 at.% peak burnup level since no deleterious fuel/cladding chemical interaction was observed between the U-10Zr fuel and the 20% cold-worked D9 cladding. Some sensitization of the cladding (grain boundary carbide precipitation) could be seen in the electroetched cladding micrographs (particularly above core midplane). No evidence for fuel/cladding mechanical interaction such as bulges or cracks in the cladding was found, even though the U-10Zr fuel is in intimate contact with the cladding inner wall at all elevations.

2. U-8Pu-10Zr. Figure 5 shows the composite metallographic sections for the U-8Pu-10Zr fuel element. Unlike the U-10Zr fuel, fuel/cladding gap-closure is incomplete at the top of the fuel slug. Approximately 0.25 mm (0.01 in.) of diametral clearance is still available for fuel swelling accommodation. The lack of pronounced fuel plasticity at the bottom closure plug is also at variance with the observed U-10Zr fuel behavior but is consistent with the appearance of three or four small radial cracks which have apparently initiated at the fuel surface and grown about 0.25 mm (0.01 in.) inward toward slug center at the bottom of the column. The lower longitudinal section shows that some fuel pin "liftoff" has occurred. Liftoff is a term to describe the displacement of the fuel slug above the lower closure plug. The liftoff shown amounts to about 0.3 mm (.012 in.). No liftoff was observed in any of the U-10Zr fuel but minor liftoff of the U-8Pu-10Zr and U-19Pu-10Zr fuel at 2.1 and 2.9 at.% burnup was seen. The higher swelling rate of the U-10Zr alloy may have filled in any liftoff which had occurred at low burnup prior to the PIE. Liftoff is a common effect in Mark-II/U-5Fs fuel and is typically 2 mm (0.080 in.) in 25% of the elements examined.[2] Further liftoff in the Pu bearing fuel is not expected beyond this initial stage once fuel/cladding gap closure is completely established.

The U-8Pu-10Zr fuel, in all but the very top of the column, has been restructured into three concentric zones. At core midplane the central and outermost zones each contain about 40% areal fraction of gas bubbles. Microchemical analysis showed that the centermost zone contained fuel of approximate composition U-9Pu-14Zr. The gamma autoradiograph shown in Fig. 5 for the bottom section, qualitatively suggests a high fission product concentration in the center of the slug. This was confirmed by gamma ray spectroscopy of the EDM samples from a companion U-8Pu-10Zr element at 2.1 at.% peak burnup. Higher than average activity from ^{95}Zr, ^{95}Nb, and ^{140}La was measured. The broad middle zone has a much finer distribution of gas bubbles, with an areal coverage of about 30%. This region was found to be only slightly depleted in zirconium with respect to the nominal as-built composition. As was the case for the U-10Zr fuel, no deleterious fuel/cladding chemical or mechanical interaction could be observed.

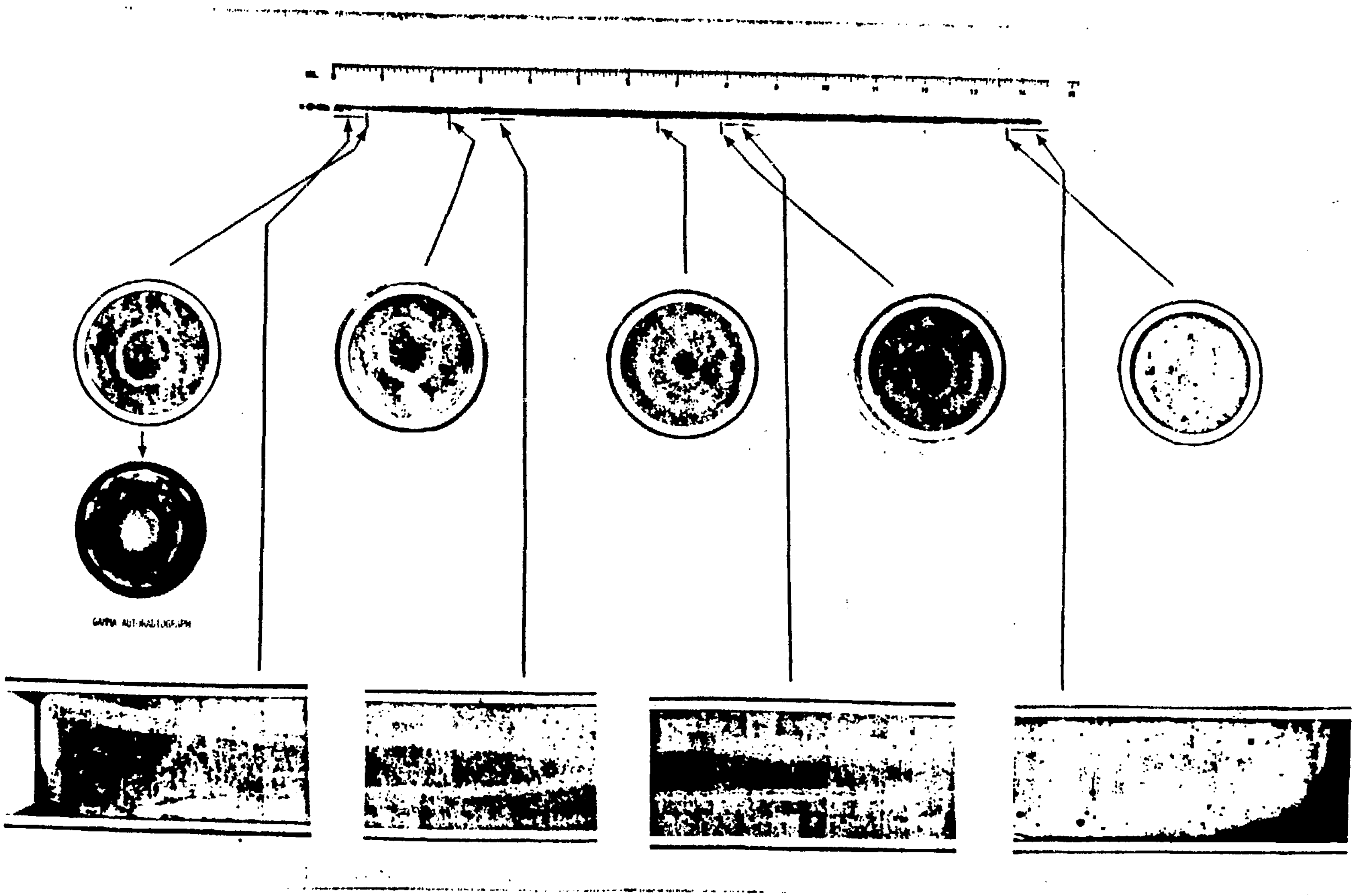

Figure 5. U-8Pu-10Zr Fuel Microstructure at 2.1 at.% Peak Burnup.

3. U-19Pu-10Zr. The most extensive fuel restructuring was observed in this alloy type. Figure 6 shows the composite micrographs at various elevations on the fuel column. The central porous zone varied in diameter along the length of the fuel column and was not always symmetrically located about fuel centerline. The location of the boundaries between the central and intermediate zones do not follow the longitudinal isotherms calculated by the heat transfer codes for beginning-of-life properties. This implies that the location of the zonal boundaries would not have been predicted by considering ternary phase equilibria only. A transverse micrograph of the fuel at 60 mm (2.4 in.) above the core midplane is shown in Fig. 7 depicting the usual three zone structure. At core midplane the porous central zone contains about 40 to 50% areal coverage of gas bubbles. Beta-gamma autoradiographs show the central zone to be the most active, suggesting a high fission-product content in this region. A companion U-19Pu-10Zr element was found to contain high ^{95}Zr, ^{95}Nb, ^{140}La, ^{141}Ce, and ^{144}Ce activity in the center of the slug at the bottom of the element. The dense intermediate zone contains large radially-oriented columnar grains which are essentially free of fission gas bubbles (5 to 10 % areal fraction). The bubbles that do form in this zone decorate the grain boundaries and link up to form grain boundary cracks. Coalescense of these cracks at the boundary between the intermediate and outer zone creates an interlinked annular network of porosity. Irregular pie-shaped cracks can be seen in the outer fuel zone at all elevations on the fuel column. The azimuthal location of these cracks bears no relationship to spacer wire orientation and appear to have nucleated sometime early in life judging by the crack opening displacements at the fuel periphery. The role of thermoelastic stress in metallic fuel pin fracture is the subject of a companion paper in these proceedings.[3] Preliminary metallography on a U-19Pu-10Zr element from X419 at higher burnup (2.9 at.% peak burnup) shows that fuel swelling proceeds to fill in the pie-shaped cracks in all areas of the pin except near the top. However, the network of porosity on the outer edge of the intermediate zone has become further developed and interlinked. The structure of the U-19Pu-10Zr fuel at this burnup suggests that a higher smear density design may be tolerated since the cracks and coarse porosity remain open.

The section shown in Fig. 7 was analyzed for uranium, plutonium, and zirconium using the electron microprobe. The raw microprobe traces obtained in a scan across the fuel slug radius are shown in Fig. 8. The correspondence between the zirconium signal and fuel microstructure suggests the dense intermediate zone to be zirconium-depleted. This was confirmed by spectrophotometric analysis of discrete EDM samples collected across the diameter of a companion element sectioned near midplane. The intermediate zone composition was found to be U-17Pu-6Zr while the zirconium-enriched centermost zone contained 18% plutonium and 16% zirconium. Two samples taken at ~0.75 X/R yielded fuel of average composition U-17Pu-13Zr.

No evidence for deleterious fuel/cladding chemical or mechanical interaction was found.

C. Fission Gas Behavior

Because low smear-density design reduces fuel/cladding mechanical interaction, but allows high rates of fission gas release, the amount of fission gas released to the plenum is an important performance parameter. The stress in the cladding wall depends not only on the gas release but on the

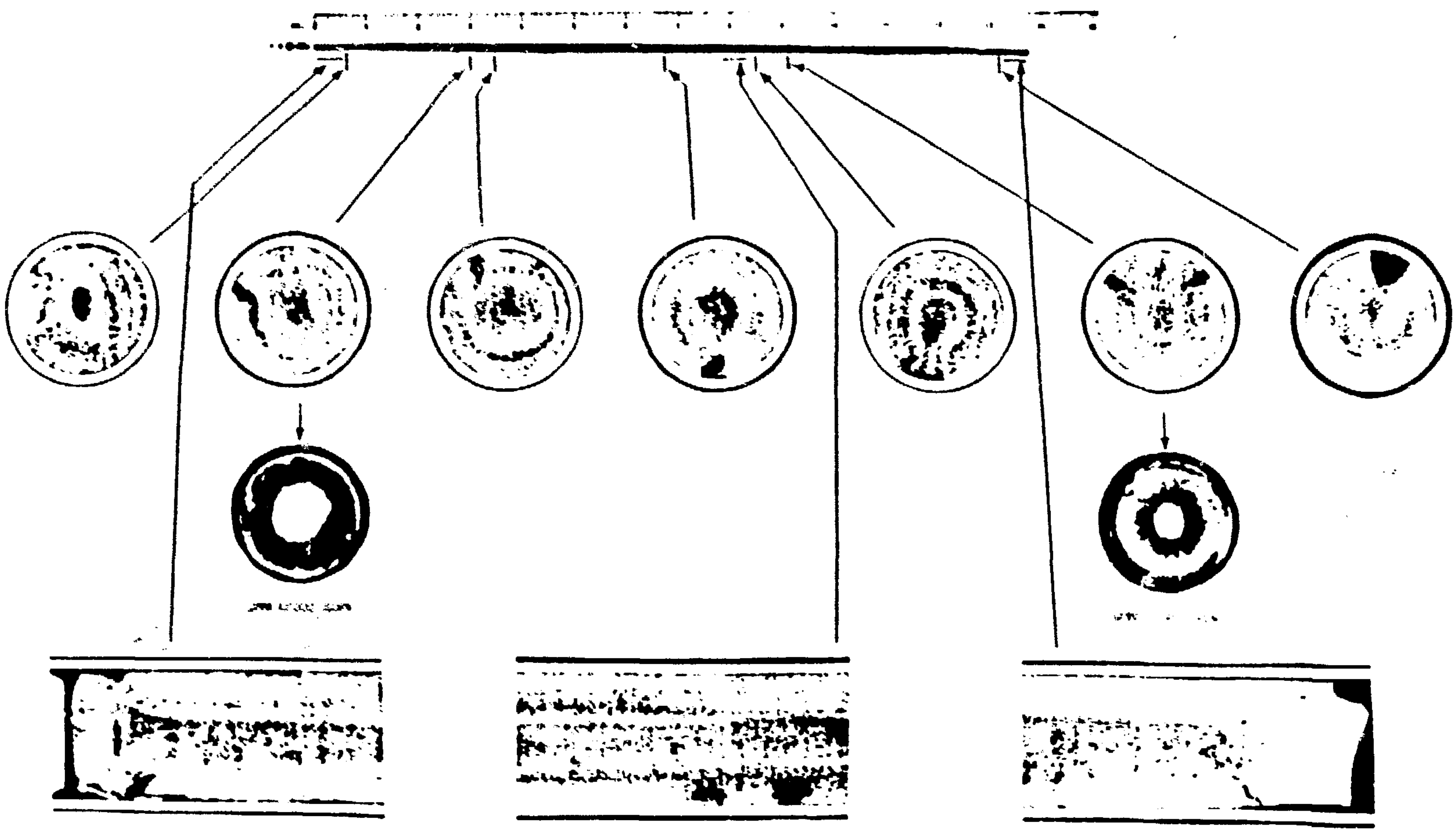

Figure 6. U-19Pu-10Zr Fuel Microstructure at 2.1 at.% Peak Burnup.

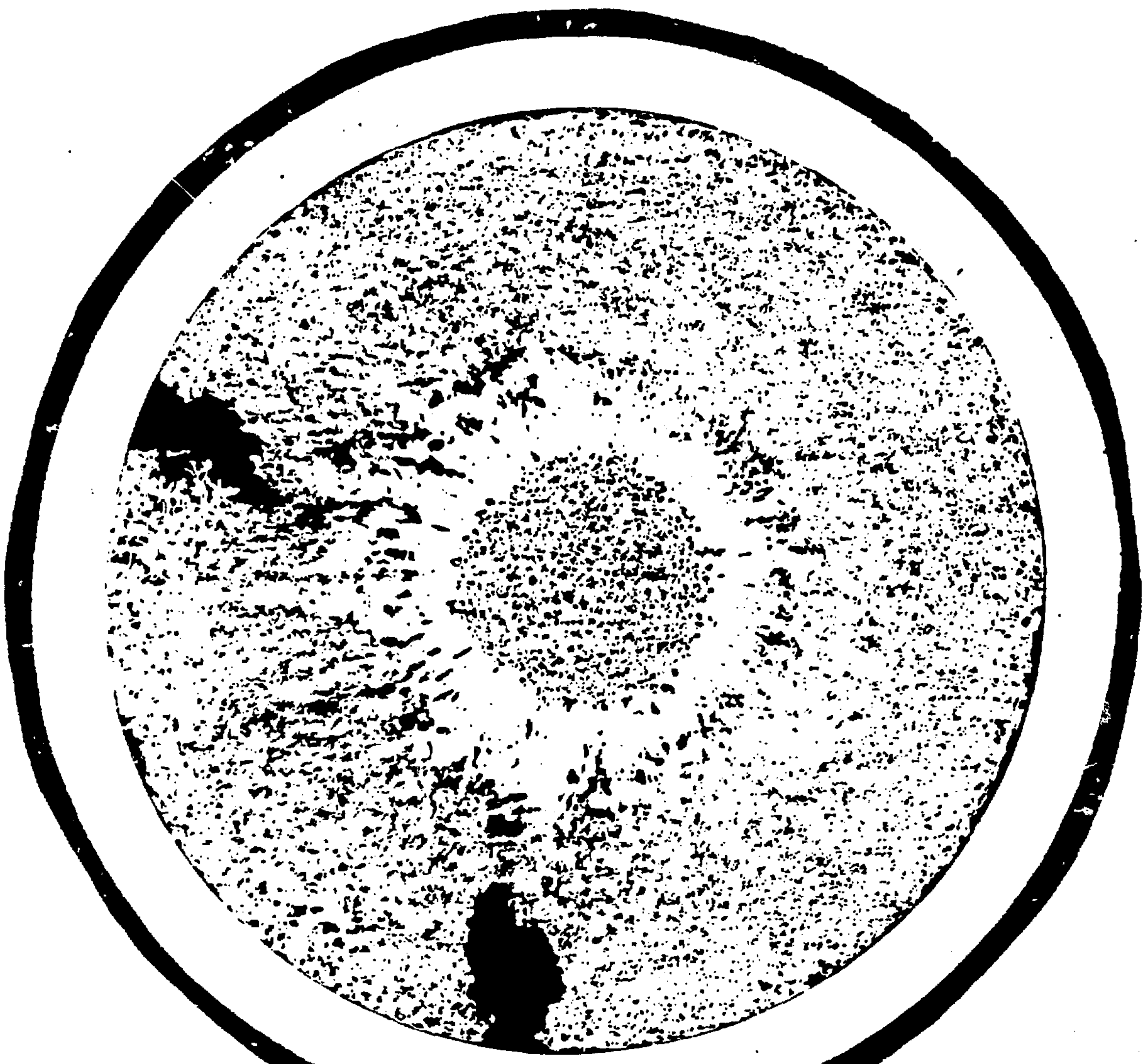

Figure 7. Transverse Section of the U-19Pu-10Zr Fuel (2.1 at.% Peak Burnup) at X/L = 0.67.

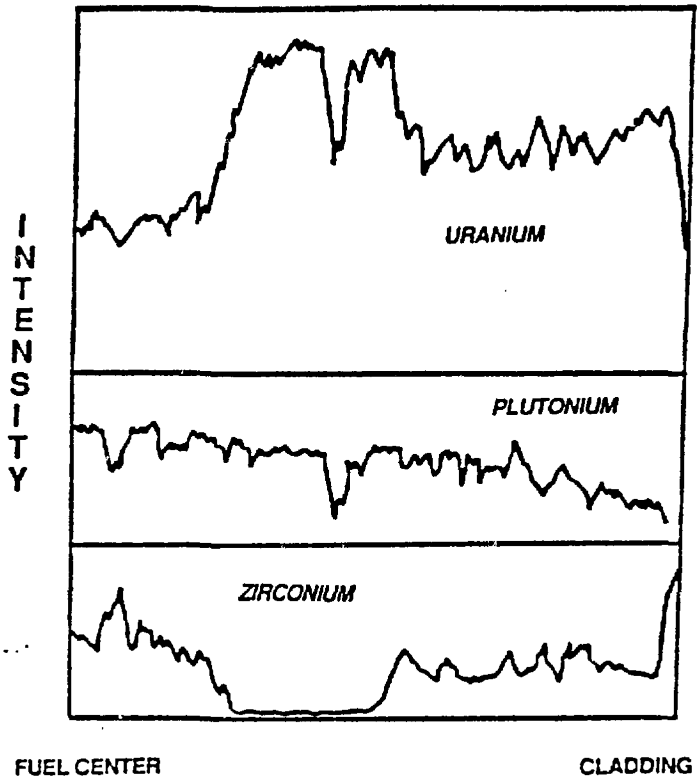

Figure 8. Uncorrected Radial Microprobe Traces of the U-19Pu-10Zr Fuel Shown in Figure 7.

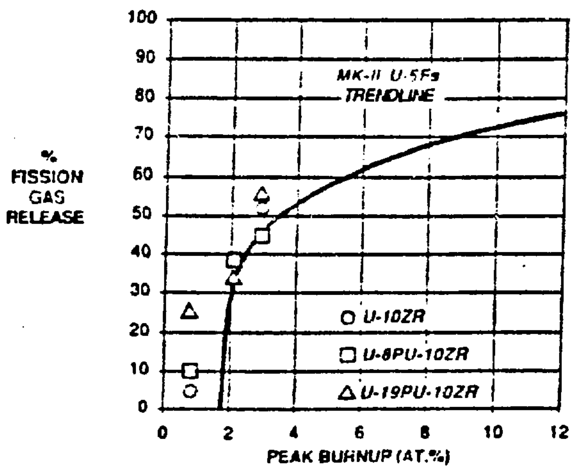

Figure 9. Burnup Dependence of Fission Gas Release.

available plenum volume as well. Initial fuel swelling and thermal expansion displaces the annulus sodium into the plenum, reducing its volume from the as-built condition. However, once interconnected porosity develops, the plenum is once again increased by virtue of bond-sodium infiltration into the fuel. Rough estimates of bond sodium content in the fuel region have been made by interpretation of neutron radiographs. At 2.9 at.% peak burnup room temperature measurements showed that the U-10Zr fuel had about 34% of its fission gas bubble volume filled with sodium. Estimates of sodium infiltration in the plutonium-bearing fuel is not so straightforward due to the presence of radial cracks and the still open fuel/cladding gap near the top of the slug.

The ratio of the number of moles of stable fission gas isotopes present in the plenum to that produced by burnup was determined by puncturing the element in the hot cell and measuring the quantity of gas which escapes. This ratio is plotted in Fig. 9 for the three alloys from subassembly X419 along with the MK-II U-5Fs trendline from reference 4. Good agreement between the two sets of data exists though the Mark-II U-5Fs trend-line lies somewhat below the experimental data we have plotted. This may be due to the lower-swelling rate of the U-5Fs fuel. The high gas release shown for the U-19Pu-10Zr fuel at 0.81 at.% peak burnup would not be expected by geometric considerations since the degree of bubble interconnectedness, and hence release, should be a strong function of fuel swelling magnitude. Since the 19% plutonium alloy swells the least of all three experimental alloys, the radial cracks present in the fuel at this burnup level may be facilitating gas transport. Because fuel deformation is driven principally by fission gas bubble pressure, experiments were performed to measure the amount of retained fission gas present in the fuel at 2.1 at.% peak burnup. Two different approaches to the problem were taken. The first involved the dissolution of 6.4 mm (0.25 in.) sections of fuel which has been mechanically pushed out of their cladding. The fuel was dissolved and three samples at top, middle, and bottom of the U-19Pu-10Zr fuel were taken. Total gas retention measurements (Xe plus Kr by isotopic dilution mass spectrometry) yielded 25%, 16%, and 18%, respectively. The second technique (discussed in reference 5) involved melting a section of the fuel with cladding intact, collecting the gas in a cold trap and measuring its volume. This method yielded retention fractions of 40%, 24%, and 23% of the average gas produced, uncorrected for local burnup. While both methods showed highest retention at the top of the slug, the gas release data of Fig. 9 implies that about 65% of the gas should be still in the fuel column at this burnup. Further work is needed to clarify how much gas may be lost during sample preparation and storage and what fraction of gas resides in the open porosity and cracks.

Plenum pressures in-reactor were calculated from the 2.9 at.% peak burnup data for subassembly X419 (Fig. 9). Corrections were made to the measured plenum volumes for sodium expansion at temperature. The resulting pressures for the U-10Zr, U-8Pu-10Zr, and U-19Pu-10Zr fuel yielded 3.2 MPa (464 psi), 2.8 MPa (406 psi), and 3.1 MPa (450 psi), respectively. These pressures are comparable to those calculated for Mark-II/U-5Fs driver elements at equivalent burnup, as discussed in the companion paper by Porter, et al.[6]

Helical profilometery measurements of the D9 cladding with spacer wire intact were made to determine the diametral strain due to swelling and creep in the fuel elements at 2.9 at.% peak burnup in X419. The maximum increase in cladding diameter at 2.9 at.% burnup was approximately 0.018 mm

(0.0007 in.) over nominal (.30% strain). No correlation between fuel alloy type and cladding strain profile could be made at this low level of fluence.

IV. FUTURE TEST PLANS

Post-irradiation examinations of subassemblies X419 and X423 are an ongoing effort, and the data presented in this paper summarizes only initial results. The five subassemblies in this test program will be irradiated to first cladding breach with the exception of X423 which will be terminated at 5 at.% burnup. Interim examinations are planned for X420 at ~6 at.% peak burnup and for X425 at 3 at.% peak burnup. Future tests planned for EBR-II include a prototypic 37-pin driver subassembly with 7.37 mm (0.290 in.) HT9 cladding, as well as a large diameter HT9 clad 19-pin blanket fuel test using 9.40 mm (0.370 in.) diameter cladding. A 169-pin test containing U-10Zr, U-8Pu-10Zr, and U-19Pu-10Zr fuel encapsulated in 6.86 mm (0.270 in.) D9 cladding will begin irradiation in the FFTF reactor at Hanford, Washington in September 1986. This test utilizes a 36-in. enriched fuel column and will operate at a beginning-of-life PCT of 616°C for 10 at.% burnup.

V. ACKNOWLEDGMENTS

The authors wish to acknowledge the contributions made by the EBR-II Fuels and Materials Department, personnel of REE Division at the Hot Fuels Examination Facility and the personnel of the Analytical Chemistry Department at ANL (Idaho). The technical support provided by the ANL MST Division at the Alpha Gamma Hot Cell Facility in Illinois is also greatly appreciated.

VI. REFERENCES

58774 Summ.

1. B. R. Seidel, et al, Experience with EBR-II Driver Fuel, this conference.

2. G. L. Hofman, Irradiation Behavior of Experimental Mark-II Experimental Breeder Reactor II Driver Fuel, Nuclear Technology, 47, 7 (1980). 40893

3. M. C. Billone, et al, Status of Fuel Element Modeling Codes for Metallic Fuel, this conference.

4. R. E. Einziger and B. R. Seidel, Irradiation Performance of Metallic Driver Fuel in Experimental Breeder Reactor II to High Burnup, Nuclear Technology, 50, 25 (1980). 43094

5. G. R. Fenske, et al, Fission Gas Retention and Axial Expansion of Irradiated Metallic Fuels, this conference.

6. D. L. Porter, et al, Factors Controlling Metal Fuel Lifetimes, this conference. 59893